Compactification of Nonlinear Patterns and Waves

Philip Rosenau and Eugene Kashdan
*School of Mathematical Sciences Tel Aviv University, Tel Aviv 69978, Israel**
(Received 30 June 2008; published 22 December 2008)

We present a nonlinear mechanism(s) which may be an alternative to a missing wave speed: it induces patterns with a compact support and sharp fronts which propagate with a finite speed. Though such mechanism may emerge in a variety of physical contexts, its mathematical characterization is universal, very simple, and given via a sublinear substrate (site) force. Its utility is shown studying a Klein-Gordon $-u_{tt} + [\Phi'(u_x)]_x = P'(u)$ equation, where $\Phi'(\sigma) = \sigma + \beta\sigma^3$ and endowed with a subquadratic site potential $P(u) \sim |1 - u^2|^{\alpha+1}$, $0 \le \alpha < 1$, and the Schrödinger $iZ_t + \nabla^2 Z = G(|Z|)Z$ equation in a plane with $G(A) = \gamma A^{-\delta} - \sigma A^2$, $0 < \delta \le 1$.

DOI: 10.1103/PhysRevLett.101.264101 PACS numbers: 05.45.Yv, 03.75.Lm, 42.81.Dp, 52.35.Sb

Introduction.—With a few notable exceptions such as the electromagnetic or acoustic waves, the majority of model equations describing waves in complex systems, whether a Gaussian response to a thermal source, or solitary waves in solids, beget patterns plagued by infinite precursors. This may be a reflection of our limited modeling ability and/or shortcoming of mathematics to describe physics.

However, one may reverse the issue and on a fundamental level inquire whether there are alternative mechanisms to the missing characteristic wave speed which also induce waves with a sharp front and a compact support. Since, mathematically speaking, on the front of such a wave analyticity is lost, the prospective mechanism(s) has to induce singular features which break the analytical spell of waves like solitons which, in spite of being localized, extend indefinitely. To see how those dictates may translate into physics, let us consider a simple setting of diffusion and radiation in plasma

$$T_t = [D(T)T_x]_x - \gamma T^m, \qquad \gamma \ge 0, \tag{1}$$

T is the temperature and $D(T)$ a coefficient of thermal diffusion. If $D(T) > 0$ and $m > 1$, Eq. (1) describes a conventional diffusive-radiative process. Let us first ignore radiation, $\gamma = 0$, but assume $D(T) \sim T^n$, $n > 0$, ($n = 5/2$ in a fully ionized case); then at the ground state $D(T)$ degenerates. This induces thermal waves with sharp fronts that expand at a finite speed into the cold ambience, rather than the usual immediate spread [1]. Projecting the compacting effect of degeneracy elsewhere, one finds that a degenerating nonlinear dispersion may induce compactons: solitary waves with a compact support [2], say, due to vibrations in a genuinely anharmonic mass-spring chain [3], particles dispersion in suspension [4], compression along a chain of colliding hard balls [5] or migration of magma [6]. These diverse phenomena have a common mathematical thread: degeneracy of the leading order operator causes a local loss of uniqueness on a singular manifold which enables to tie the solution with its trivial counterpart and thus form a robust compact entity in one, [2,3], or N-dimensions [7].

We now let $D(T)$ be constant and restore the radiation but, as in the bremsstrahlung radiation where $m = 1/2$, assume that $m < 1$. The resulting sublinear radiation effectively arrests the immediate spread of initial disturbance yielding a pattern that propagates with a finite speed. Once again, the singularity due to sublinearity causes a local loss of uniqueness and thus enables to tie the solution with the trivial ground state.

We may induce the compactifying effect of the sublinear force in a variety of otherwise completely different processes like those described by, say, the Klein-Gordon, and Schrödinger equations. Endowing their dynamics with such a force yields solitary waves with a compact support. One may thus say that irrespective of its origin, a mechanism capable of inducing a local loss of uniqueness, can induce compact patterns. In this respect, note a similar effect due to a sublinear convection [8] and the very different nature of the dissipative-radiative, Eq. (1), and the dispersive processes to be presented next.

C-KG.—We start with a non-linear Klein-Gordon model viewed as a continuum limit of an anharmonic mass-spring chain embedded in a site potential $P(u)$

$$-u_{tt} + [\Phi'(u_x)]_x = P'(u), \tag{2}$$

where $\Phi'(\eta) = \eta + \beta\eta^3$ and

$$P(u) = \frac{1}{2(1+\alpha)}|1 - u^2|^{1+\alpha} \quad \text{and} \quad 0 \le \alpha < 1. \tag{3}$$

Let $s = x \mp \lambda t$; then two integrations reduce the problem into a motion in a potential well $V(u;\beta)$,

$$\frac{1}{2}\omega^2 u_s^2 - V(u;\beta) = 0, \qquad V \equiv P(u)P_\beta(u), \tag{4}$$

where $\omega^2 \equiv 1 - \lambda^2$ and P_β is due to anharmonicity

$$P_\beta(u) = \frac{2}{1 + \sqrt{1 + 12\beta P(u)/\omega^4}}. \tag{5}$$

We start with the harmonic, $\beta = 0$, case. Now

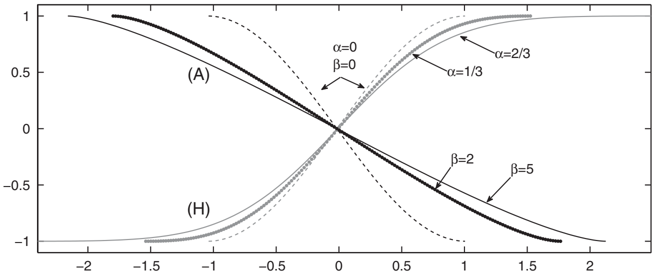

FIG. 1. (H) Impact of α on kinks shape and width for $\beta = 0$. (A) Impact of anharmonicity parameter β/ω^4 for $\alpha = 0$. In all cases, $\lambda = 0.90$ and $\omega = \sqrt{1-\lambda^2} \approx 0.436$.

$$\omega^2 \theta'^2 = \frac{1}{1+\alpha} \cos^{2\alpha}\theta, \quad \text{where } u = \sin\theta. \tag{6}$$

$$\text{thus } I(\alpha, \theta) \equiv \int_{-\pi/2}^{\theta} \frac{d\theta}{\cos^{\alpha}\theta} = \pm \frac{s}{\omega\sqrt{1+\alpha}}. \tag{7}$$

If $\alpha = 1$, the topological soliton $u = \pm \tanh(s/\omega\sqrt{2})$ has an infinite support, but for $\alpha < 1$, the integral converges and $|1 - u^2| \sim x^{1/1-\alpha}$ at the edges. The $u = \mp 1$ gap is now spanned by a kink of a finite width

$$L = \omega\sqrt{1+\alpha} I(\alpha, \pi/2). \tag{8}$$

Differently stated, a hetroclinical orbit connects the two, ∓ 1, states in a "finite" time. Thus, the compact span of kinks (hence the "C" in the title) is due to the subquadratic nature of $P(u)$. For $\alpha = \beta = 0$,

$$u = \begin{cases} +1 & s/\omega \geq +\pi/2 \\ \pm\sin(s/\omega) & -\pi/2 \leq s/\omega \leq \pi/2 \\ -1 & s/\omega \leq -\pi/2 \end{cases} \tag{9}$$

and $P'(u) = -u \,\mathrm{sgn}(1 - u^2)$ is now piecewise linear.

For $\alpha \neq 0$, kinks profiles follow from Eq. (7), see (A) in Fig. 1. Before we turn to describe interaction of kinks, we stress that their nonanalyticity precludes the standard perturbation approach which anyway would not carry over to the nonlinear stage. Equation (2) was integrated using a fourth order scheme in space and time with a dissipative smoothing, ϵu_{txxxx}, $\epsilon = \mathcal{O}(10^{-5})$, of the short wavelengths.

In Figs. 2–4, we describe a head-on ($><$) and chasing interactions ($\gg$) on a periodic domain of two $\beta = 0$, kinks, see Eq. (7). These and other interactions are snapshots of movies available in [9]. In general, motion of a single kink is robust, but there is some momentum transfer during kinks interaction. We found the $\alpha = 2/3$ and $\lambda_2 - \lambda_1 = 0.25$ chasing ($\gg$) interactions to be remarkably clean, see Fig. 2, but this is more of an exception than a rule. Typically, after repeated collisions, kinks may both fuse and decompose and form one or few traveling quasi-breathing formations of compact support pulsating sporadically, see Fig. 3. Occasionally, after a few head-on, $><$, encounters, two kinks may "synchronize" and form a traveling pair which propagates in the same direction and

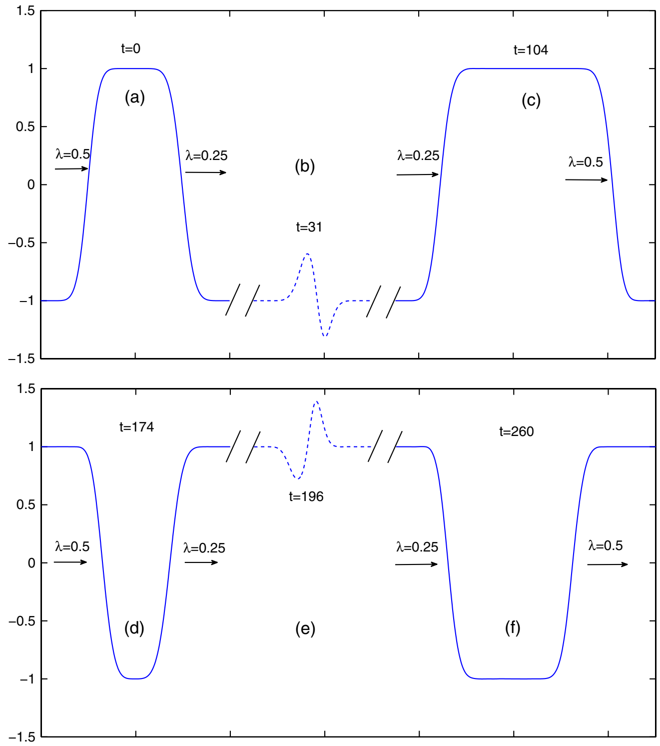

FIG. 2 (color online). A remarkably clean $\gg$ interactions of two, $\alpha = 2/3$, $\lambda = 0.50$, and $\lambda = 0.25$ kinks. Here and elsewhere periodic boundaries were used.

expands slowly with slightly wobbling fronts, see cases (d) and (e) in Fig. 4.

We reiterate the crucial role of the subquadratic part of the potential near its edges. Other features impact its shape but not compactness. Thus, if in the sine-Gordon set up we take $P(u) = -|\cos u_0 - \cos u|$ but with $0 < |u_0|$, the cusps thus induced beget compact kinks. In a mechanical realization, this would represent a chain of spring coupled pendulums reflected before reaching the top. We note that the $\alpha = 0$ case in (3) may also follow from a Josephson chain of superconducting wires [10].

Anharmonicity.—Restoring β widens the kinks, see part (A) of Fig. 1, which remain robust though their interaction causes their demise. Note the mollifying effect of the substrate force without which the nonlinear stress in

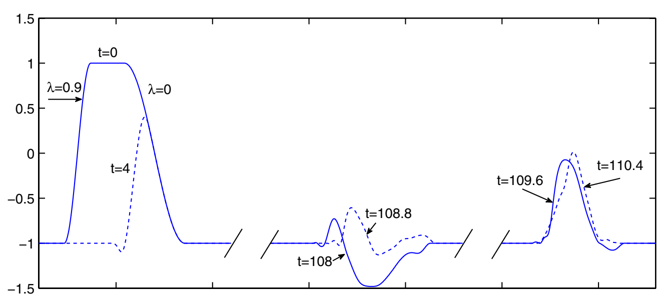

FIG. 3 (color online). A typical collision scenario. After 3 collisions, the $\lambda = 0.90$ and the stationary, $\lambda = 0$, kinks fuse into a quasibreathing formation $\alpha = 0$.

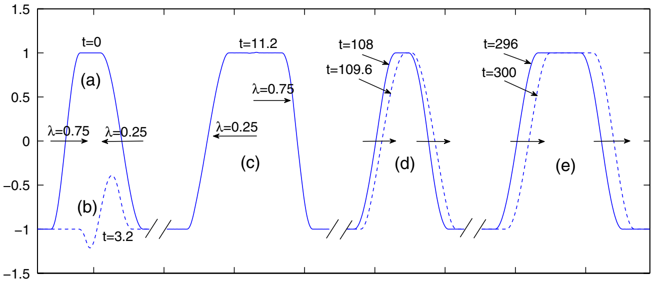

FIG. 4 (color online). Two, $\alpha = 0$, kinks before, (a), during, (b), and after, (c), one collision. After the third collision, $t \sim 79$, kinks start to "synchronize" into a traveling formation which, see (d), (e), widens and, due to an artificial dissipation used in all simulations of the C-KG, decelerates slowly [in (d) velocity $\sim$0.37 and in (e) $\sim$0.30]. Since, see (d) and (e), the fronts wobble a bit the motion is not a pure translation.

Eq. (2) turns unbounded [11]. A similar effect was also found in the continuum limit of a strictly anharmonic mass-spring chain [3]. The resulting compact breathers, see also [12], help one to realize that their singularities are a trace of a very narrow boundary layer on a lattice wherein the tails decay in a doubly exponential rate. In the limit, these layers shrink into a singularity that defines compactons edge.

C-NLS.—We now turn to the Schrödinger equation

$$iZ_t + Z_{xx} = (\gamma|Z|^{-\delta} - \sigma|Z|^2)Z, \qquad 0 < \delta \leq 1. \quad (10)$$

As in the C-KG case, the sublinearity induces a solitary waves with a compact support, and hence the "C" in its title. We seek a modulated traveling wave

$$\mathbf{Z} = A(s)\exp[i(ls + \Omega t)] \quad \text{where } s = x - \lambda t. \quad (11)$$

From Eqs. (10) and (11), one deduces

$$A'' + \kappa^2 A - \gamma A^{1-\delta} = -\sigma A^3, \quad (12)$$

provided that we take

$$l = \lambda/2 \quad \text{and} \quad \Omega = \lambda^2/4 - \kappa^2 \quad (13)$$

and κ is a modulation parameter. Naturally, we start with the $\sigma = 0$ case. From Eq. (12),

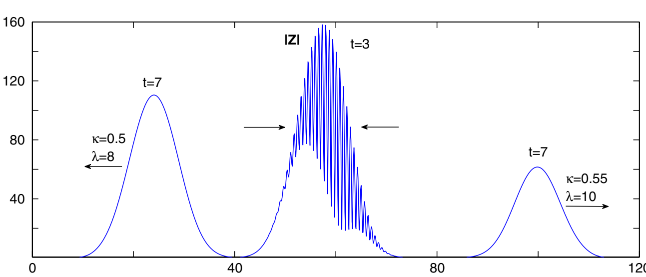

FIG. 5 (color online). A head-on collision and reemergence of two C-NLS, $\sigma = 0$, $\delta = 1/3$, envelope compactons. The modulations throughout interaction are genuine and not a numerical artifact. Note the sensitive dependence of $\mathbf{Z}$ on κ, see Eq. (14).

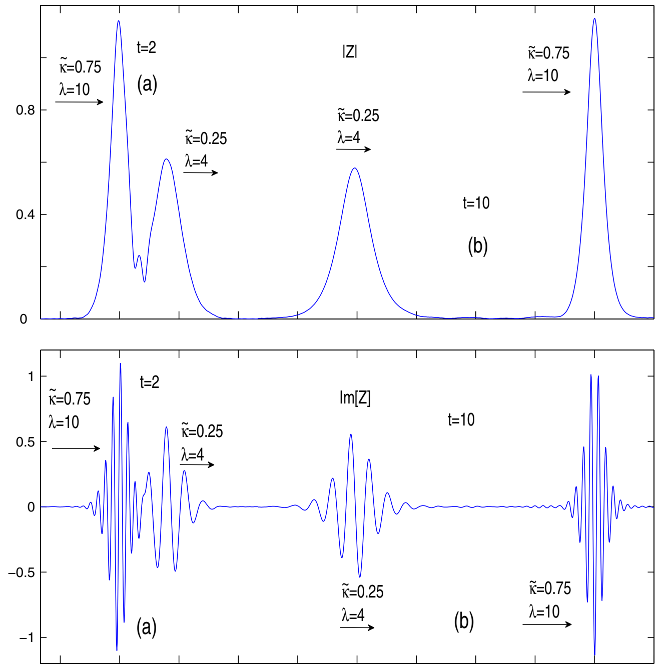

FIG. 6 (color online). Two, $\sigma = 1$, $\delta = 1/3$, C-NLS compactons during and after interaction. For $\gamma = 0.1$ compactons pattern, except for the vicinity of edges, is similar to that of the pure NLS soliton.

$$\mathbf{Z} = \left[\frac{2\gamma}{(2-\delta)\kappa^2}\right]^{1/\delta} \cos^{2/\delta}\left(\frac{\kappa\delta}{2}s\right)\exp[i(ls + \Omega t)], \quad (14)$$

for $|s| \leq \pi/(\delta\kappa)$ and vanishes elsewhere. The number of modulations within the compact pulse is finite and increases with λ. Figure 5 displays $|\mathbf{Z}|$ during an interaction of two $\delta = 1/3$ compactons. They are robust, and as δ decreases, their interaction becomes more, though not entirely, elastic. The amplitude modulations seen during compactons interaction describe a real effect and is not a numerical artifact. This was confirmed quadrupling the number of points of integration. Unlike the Klein-Gordon case, no artificial dissipation was used to integrate Eq. (10).

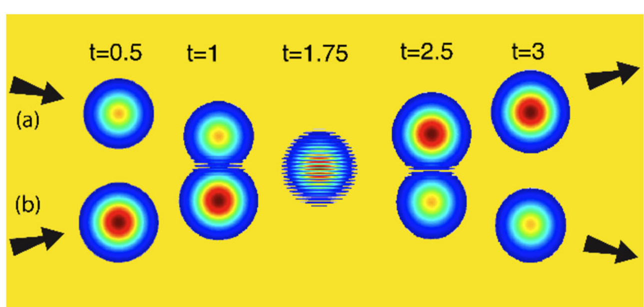

FIG. 7 (color online). Support of two compactons colliding at 60°. Note the sense of direction of each compacton. The inelastic effect becomes noticeable only after 10 collisions. A collision at 120° yields a similar scenario but in a reverse direction. Here, $\gamma = 1$, $\delta = 1/3$, $\sigma = 0$, $\kappa_a = 0.80$, and $\kappa_b = 0.75$.

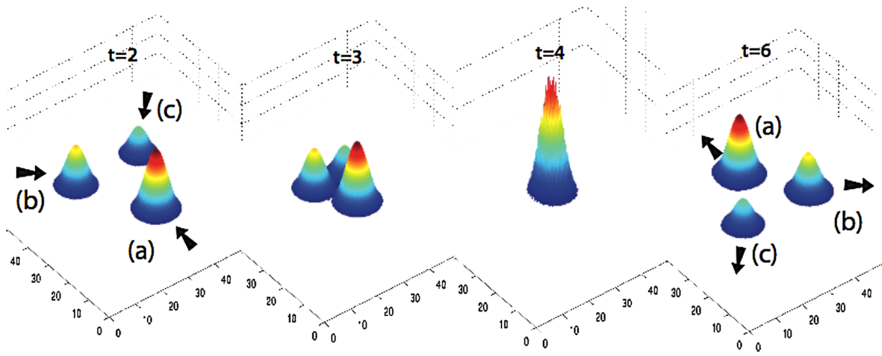

FIG. 8 (color online). Amplitudes of three interacting C-NLS compactons with $\kappa_a = 0.85$, $\kappa_b = 0.80$, $\kappa_c = 0.75$, and $\lambda = 7$. They reemerge unchanged keeping their sense of direction. Here, $\sigma = 0$, $\gamma = 1$, and $\delta = 1/3$.

For $\sigma \neq 0$, A is given implicitly via

$$\frac{\delta}{2} s = \int_0^{A^{\delta/2}} \frac{dY}{\sqrt{\frac{2\gamma}{2-\delta} - Y^2(\kappa^2 + \frac{\sigma}{2} Y^{4/\delta})}}. \qquad (17)$$

To see impact on the standard NLS solitons, let $\kappa^2 \to \tilde{\kappa}^2 = -\kappa^2$, $\delta = 1/3$, and $\sigma > 0$. Now, σ controls the amplitude of the compacton which hardly depends on $\tilde{\kappa}$. For the core of the compacton to look NLS-like, for $\sigma = 1$ one takes $\gamma = 0.1$, see Fig. 6.

C-NLS on a plane.—Let $Z_{xx} \to \nabla^2 Z$ in (10). Seeking radial compactons moving in x-direction, we set $A(s) \to A(R = \sqrt{s^2 + y^2})$ in (11). This yields

$$\frac{1}{R}\frac{d}{dR} R \frac{dA}{dR} + \kappa^2 A - \gamma A^{1-\delta} = -\sigma A^3. \qquad (16)$$

Note that since the choice of the x-axis is arbitrary, each compacton may propagate in any direction. For $\sigma = 0$, Eqs. (12) and (16) scale as $A_\kappa(R) = \kappa^{-(2/\delta)} A_1(\kappa R)$, tall compactons are thus wide cf. Fig. 8. This should be contrasted with the *NLS* scaling $A_\kappa(R) = \kappa A_1(\kappa R)$. For $\delta - 1 = \sigma = 0$, we obtain an explicit form

$$A = \frac{\gamma}{\kappa^2}\left[1 - \frac{J_0(\kappa R)}{J_0(\kappa R_*)}\right], \qquad 0 < R \leq R_*, \qquad (20)$$

and vanishes elsewhere. $R_* = r_1/\kappa$ and r_1 is the first nonzero root of J_1. In Figs. 7 and 8, we describe collisions of two and three $\sigma = 0$ radial C-NLS compactons obtained solving (16) with compactons preserving their original direction after a collision. For $\delta = 1/3$, collisions are quite clean, but the collisions inelasticity increases with δ. When $\sigma \neq 0$, as in the pure NLS case, the planar compactons are unstable. For movies of these and other patterns, see [9].

Discussion.—That the C-NLS, Eq. (10), may be viewed as a complex extension of Eq. (1) attests to the power of analogies. Clearly, the underlying physical processes and the resulting patterns are quite different, and yet the sublinear force is equally effective in both cases in enforcing compact patterns with sharp fronts. With respect to the nonanalyticity of such fronts, or for that matter any front, we note that our ease with analyticity is more a by-product of our scientific upbringing than a reflection of reality. In this respect, we recall the "nonanalytical" nature of Hertz force between colliding spheres [5] or the Van der Waals force at the edge of a liquid drop [8]. Though we have indicated two possible applications for the C-KG type equations, our goal was not to address a particular setup, or to speculate about the possible use of the C-NLS compactons in optics, but to use the two models, with the target function being either scalar or a vector, as a launching platform for the new concept and thereby challenge the reader to find her or his own applications. Finally, we note a subtle difference: while in the C-NLS, the sublinearity provides an alternative to a missing characteristic speed; in the C-KG, which has a natural light cone, it enables translation of kinks of compact support.

This work was supported via the I. S. F Grant No. 801/07. The first author was also supported in part via the US NSF No. DMS-07-0785. We thank Professor M. Karliner for his interest and comments.

*rosenau@post.tau.ac.il

[1] G. I. Barenblatt, *Scaling, Self-Similarity and Intermediate Asymptotics* (Cambridge University Press, Cambridge, England, 1996).
[2] P. Rosenau and J. M. Hyman, Phys. Rev. Lett. **70**, 564 (1993); P. Rosenau, Notices of the American Mathematical Society **52**, 738 (2005); P. Rosenau, Phys. Lett. A **356**, 44 (2006).
[3] P. Rosenau and S. Schochet, Phys. Rev. Lett. **94**, 045503 (2005).
[4] J. Rubinstein, Phys. Fluids A **2**, 3 (1990).
[5] V. F. Nesterenko, *Dynamics of Heterogeneous Materials* (Springer-Verlag, New York, 2001); C. Coste, E. Falcon, and S. Fauve, Phys. Rev. E **56**, 6104 (1997).
[6] G. Simpson, M. Spiegelman and W. I. Weinstein, Nonlinearity **20**, 21 (2007); M. Nakayama and D. P. Mason, J. Phys. A **27**, 4589 (1994); V. Barcilon and O. Lovera, J. Fluid Mech. **204**, 121 (1989).
[7] P. Rosenau, J. M. Hyman, and M. Staley, Phys. Rev. Lett. **98**, 024101 (2007).
[8] P. Rosenau, Phys. Rev. Lett. **99**, 234102 (2007).
[9] http://www.math.tau.ac.il/~compact.
[10] G. Refael and P. Rosenau (to be published).
[11] W. A. Strauss, *Partial Differential Equations* (John Wiley, New York, 1992).
[12] P. Rosenau and A. Pikovsky, Phys. Rev. Lett. **94**, 174102 (2005); K. Ahnert and A. Pikovsky (to be published).